CORROSION SCIENCE AND TECHNOLOGY, Vol.2, No.2(2003), pp.82~87

Stress Corrosion Cracking of Alloy 600 and Alloy 690 in Caustic Solution

Hong Pyo Kim, Yun Soo Lim, and Joung Soo Kim

Korea Atomic Energy Research Institute, Yusong, Taejon, Korea

Stress corrosion cracking of Alloy 600 and Alloy 690 has been studied with a C-ring specimen in 1%, 10% and 40% NaOH at 315℃. SCC test was performed at 200 mV above corrosion potential. Initial stress on the apex of C-ring specimen was varied from 300 MPa to 565 MPa. Materials were heat treated at various temperatures. SCC resistance of Ni-χCr-10Fe alloy increased as the Cr content of the alloy increased if the density of an intergranular carbide were comparable. SCC resistance of Alloy 600 increased in caustic solution as the product of coverage of an intergranular carbide in grain boundary, intergranular carbide thickness and Cr concentration at grain boundary increased. Low temperature mill annealed Alloy 600 with small grain size and without intergranular carbide was most susceptible to SCC. TT Alloy 690 was most resistant to SCC due to the high value of the product of coverage of an intergranular carbide in grain boundary, intergranular carbide thickness and Cr concentration at grain boundary. Dependency of SCC rate on stress and NaOH concentration was obtained.

Keywords *: stress corrosion cracking, Alloy 600, Alloy 690, NaOH*

1. Introduction

Stress corrosion cracking (SCC) of Alloy 600 has occurred mainly at crevice because impurities segregated into crevice due to higher temperature at crevice than bulk secondary water in secondary side of steam generator. Crevice solution pH can be acidic or alkaline depending on impurities that segregated into crevice.[1),2)] Even though recent works suggest that crevice solution be in mid-range pH or light alkaline based on the analysis of corrosion products on steam generator tubing,[3)] there is still possibility that the crevice be acidic or alkaline in steam generator.

Many kinds of steam generator tubings such as high temperature mill annealed (HT) Alloy 600, thermally treated (TT) Alloy 600, TT Alloy 690 and Alloy 800 have been used in Korean nuclear power plants. SCC of HT Alloy 600 was observed in one of Korean nuclear power plants that has been operated since 1996.[4)] Molar ratio index is about 5 in the nuclear power plant, suggesting alkaline environment in the crevice. In addition, eddy current test showed signal of denting and over expansion at tube sheet region, which seems to accelerate the SCC of steam generator tubing of the nuclear power plant. So, prediction of SCC progression becomes more and more important as plants age. Steahle reported that SCC resistance of steam generator tubings varies with heat to heat even though chemical composition and microstructure do not vary significantly.[5)] However, there are too many heats in a steam generator, it is almost impossible to test all heats in a steam generator.

In this work, SCC behaviours of an archive material, typical of steam generator tubing in each nuclear power plant, and heat treated material were studied as a function of microstructure, pH and stress.

2. Experimental

The materials were nuclear grade Alloy 600s and Alloy 690s and Ni-10Cr-10Fe alloy which was made in laboratory. Most of them have been used in Korean nuclear power plants. SN Alloy 600 and TT Alloy 600 were prepared by heat treating the as-received HT Alloy 600 at 600 ℃ for 24 Hrs and 715 ℃ for 15 Hrs, respectively. TT of HT Alloy 690 was performed at 715 ℃ for 10 Hrs. Solution anneal(SA) was carried out at 1100 ℃ for 30min. SASN and SATT stand for heat treatment of SA alloys at 600 ℃ for 24Hrs and 715 ℃ for 15Hrs, respectively. Some of the tubings were elongated by 20 % to increase yield strength of C-ring specimen. Maximum at the apex of the C-ring specimen is about 340 MPa for as received Alloy 600 while that is about 565 MPa for the 20 % cold worked Alloy 600. Even though many heats are usually used in fabricating a steam generator, speci-

Table 1. Alloy designation and chemical composition of steam generator tubings

Designation	Ni	Cr	Fe	C	S	P	B	N	Si	Cu	Al	Ti
SA010	79.7	10.5	10.1	0.02	<0.001	<0.01			0.3			0.1
HT600A	72.5	16.85	9.00	0.025	0.003	0.008	0.001	0.016	0.31	0.01	0.015	0.28
HT 600B	74.76	15.63	8.62	0.025	<0.001	0.007	0.004	0.01	0.14	0.03	0.21	0.34
HT 600C	76.11	15.29	7.57	0.026	0.001	0.008	0.004	0.004	0.15	0.015	0.23	0.32
HT 600D	75.08	15.38	8.56	0.023	0.001	0.006	0.003	0.01	0.20	<0.01	0.24	0.26
HT600	75.14	15.46	8.42	0.025	0.001	0.008	0.0039	0.0042	0.16	0.011	0.21	0.29
LT 600	74.66	15.21	9.16	0.022	0.001	0.003			0.2	0.01	0.24	0.29
TT 690E	58.9	29.57	10.54	0.02	0.001	0.009	0.004	0.017	0.22	0.01	0.019	0.26
HT690	60.39	29.66	8.90	0.017	0.001	0.005	0.0007	0.009	0.14	0.007	0.35	0.26

mens were cut from only one heat in each nuclear power plant if a tubing of the heat is available. Alloy designations and their chemical compositions are shown in Table 1. First two letters, HT, LT, SN and TT in alloy designation mean high temperature mill annealed, low temperature mill annealed, sensitized and thermally treated alloys, respectively. Three digits, 600 and 690 in alloy designation mean Alloy 600 and Alloy 690, respectively. Last letter in the alloy designation stands for nuclear power plant. SA010, which was melted and rolled in laboratory, is essentially same with Alloy 600 except Cr content.

Carbide distribution and grain boundary of Alloy 600 and Alloy 690 were examined with an SEM after etching in bromine (98.5 % methanol+1.5 % bromine) for 15sec. Cr depletion around grain boundary was examined with JEOL-2000 FXII (operating voltage 200 kV) equipped with Oxford Link (Model ISIS-5947) EDX spectrometer. TEM specimen was prepared by mechanical grinding to about 60 μm and then jet thinning in an electrolyte of 10 % perchloric acid and 90 % methanol at -40 ℃.

All test solutions was prepared by adding reagent grade chemicals to demineralized water. SCC test solutions were 1 %, 10 % and 40 % NaOH. The solution in an autoclave was deoxygenated by purging nitrogen gas into the solution and then venting a gas through water. SCC tests were performed using C-ring specimens at 200 mV above the corrosion potential. Reference electrode and counter electrode were an external Ag/AgCl electrode and Pt wire, respectively. The stress at the apex of the C-ring specimen ranged from about 300 MPa to about 565 MPa. The SCC fracture surface and cross-sectional area of the C-ring specimen were examined by both scanning electron microscope and optical microscope.

Table 2. Mechanical properties of steam generator tubings.

Alloy	Yield strength (MPa)	Tensile strength (MPa)	Elongation (%)	ASTM Grain size
HT600A	275	689	44	5.5
HT600B	244	647	47	5.0
HT600C	258	675	43	6
HT600D	255	661	44	6
HT600	255	669	44	
LT600	310	679	44	
TT690E	330	730	44	
HT 690	293	698	52.2	

Table 3. Cr concentration at grain boundary, FWHM, intergranular carbide thickness and width.

Alloy	Cr depletion		Intergranular carbide		
	Min. Cr conc. (wt.%)	FWHM (nm)	Length (μm)	Thickness (μm)	Line coverage (%)
HT600	13.2	270	0.28	0.15	28
SN600	7.3	300	0.41	0.20	89
TT600	10.5	360	0.57	0.29	80

3. Results and discussion

3.1 Mechanical properties and microstructure

Metallurgical characteristics and mechanical properties of archive materials are shown in Table 2. All HT 600s have similar grain size, discontinuous intergranular carbide distribution, yield strength, tensile strength and elongation. The grain size numbers of HT, SN and TT 600 were about 6.

Cr depletion across grain boundaries measured with TEM are summarized in Table 3. The spacing between

the edge of intergranular carbide and the edge of the EDX beam is about 60 nm to avoid EDX beam passing through intergranular carbide by beam broadening. Table 3 shows that HT 600 is slightly sensitized and SN 600 is heavily sensitized in terms of minimum Cr concentration at grain boundary and that TT 600 is partially healed by Cr back diffusion into grain boundary but has wider Cr depletion width compared to SN 600.

The distribution of intergranular chromium carbide examined after etching in bromine solution are shown in Table 3. Intergranular carbide distribution in HT 600 varies even in a grain boundary and also varies from boundary to boundary. Intergranular carbide distributions in SN 600 and TT 600 are semicontinuous and almost uniform within boundary and the variation of intergranular carbide distribution from boundary to boundary diminishes significantly compared to HT 600. Line coverage of intergranular carbide was defined as sum of intergranular carbide length divided by grain boundary length. Intergranular carbide in SN 600 is more closely spaced than that in TT 600 because nucleation of intergranular carbide is dominant over growth of intergranular carbide at 600 ℃. Thickness of the intergranualr carbide increased with heat treatment temperature. So, thickness of the intergranualr carbide in SN 600 is smaller than that in TT 600. Intergranular carbide in HT 600 is loosely spaced and thin.

3.2 Effect of Cr concentration on SCC

The effects of bulk Cr content on caustic SCC resistance of solution annealed Ni-χCr-10Fe alloys are shown in Fig.

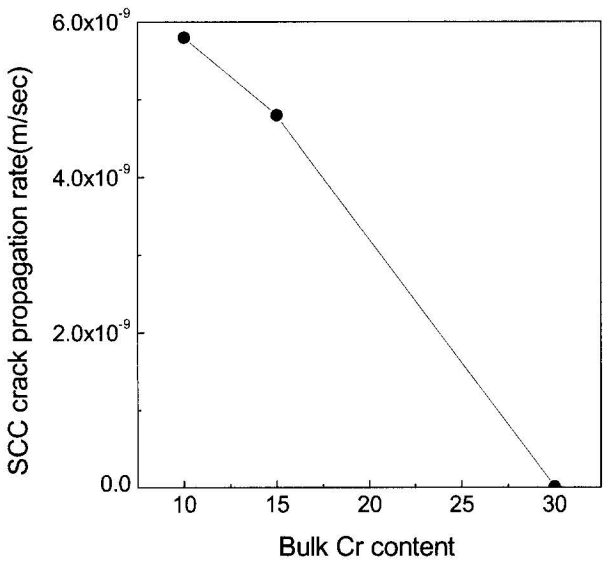

Fig. 1. Effect of bulk Cr content in Ni-χCr-10Fe alloy on SCC crack propagation rate.

1. Maximum SCC crack propagation rate was calculated by dividing maximum SCC crack length with test duration under an assumption that SCC crack initiation time is zero. SCC resistance of SA Ni-base alloy increased with increase in Cr content of SA Ni-base alloy. Enhancement of SCC resistance with an increase in Cr content was also reported for Ni base alloys tested by slow strain rate test at 900 mVsce in 50% NaOH at 140℃[5] and U-bend specimen in a deaerated 10% NaOH at 325℃.[6] These results suggest that SCC resistance of Ni-χCr-10Fe alloys increase with Cr content irrespective of test method and NaOH concentration.

Enhancement of SCC resistance of Ni-χCr-10Fe alloys with Cr content might be explained in terms of repassivation kinetics, stacking fault energy and grain boundary character distribution. Stacking fault energy of Ni decreased with addition of Cr.[7] For material with high stacking fault energy, screw dislocations are not confined to a particular plane so that stress concentration in the grain boundary is relatively low compared to that with low stacking fault energy. So, stacking fault energy of Ni may not explain the fact that SCC resistance of Ni-χ Cr-10Fe alloys increased with Cr content.

A fraction of coincidence site lattice boundary (CSLB) ($\Sigma<29$) increases with Cr content in Ni base alloys. A fraction of CSLB ($\Sigma<29$) is about 40% for a conventional Alloy 600 and about 60-70 % for a conventional Alloy 690.[8),9)] For Alloy 600, CSLB was more resistant to SCC than the general high angle boundary (GHAB) in pure water.[2)] But even GHAB of Alloy 690 are immune to SCC in pure water while CSLB of Alloy 600 was cracked.[2)] These facts implied that the CSLB is not the primary controlling factor in SCC of Ni base alloys.

Yamanaka[10)] reported that the repassivation rate and Cr enrichment in the inner layer of corrosion oxide increased with Cr content in Ni base alloy in a 4% NaOH solution at 280℃. Higher SCC resistance of Alloy 690 was attributed to a faster repassivation rate and Cr enrichment in the inner layer. However, the corrosion rate at 200 mV of Ni-χCr-10Fe alloys above the corrosion potential is increased with the Cr content in 40% NaOH at 315℃. This implies that the Cr rich inner layer of the passive film did not reduce dissolution rate, but accelerate dissolution in 40% NaOH at 315℃. So in this work the role of Cr seems to blunt the crack tip by delaying the formation of a stable film at the crack tip and thereby reduce the stress intensity factor.

3.3 SCC resistance of heat treated Alloy 600

Maximum SCC crack propagation rate are shown in Table 4 and Table 5. SCC resistance increased with a

Table 4. SCC Rate of SA Alloy 600, SASN Alloy 600 and SATT Alloy 600 in 40% NaOH at 315℃ and at a initial stress of 340MPa.

Alloy	SA Alloy 600	SASN Alloy 600	SATT Alloy 600
SCC Rate(m/sec)	4.810-9	4.010-9	0.710-9

Table 5. SCC Rate of HT600, SN 600 and TT 600 with a initial stress of and Those with a initial stress of 340MPa in 40% NaOH at 315℃.

Alloy	HT 600	SN 600	TT 600
SCC Rate(m/sec) in 10% NaOH	1.7×10^{-9}	1.3×10^{-10}	7.7×10^{-10}
SCC Rate(m/sec) in 40% NaOH	5.4×10^{-9}	3.1×10^{-9}	0.6×10^{-9}

following order: SA600, SASN600 and SATT600 for solution annealed and heat treated materials and HT600, SN600 and TT600 for high temperature mill annealed and heat treated materials. SA specimen has no intergranular carbide and so no Cr depletion around grain boundary while SATT600 has abundant intergranuar carbide and slight Cr depletion around grain boundary. So, higher SCC resistance of the SATT600 than the SA600 may be attributed to presence of the abundant intergranular carbide in SATT600. As shown in previous section, SCC resistance of Ni-XCr-10Fe alloys increased with Cr content. So, SATT600 with slight Cr depletion around grain boundary showed higher SCC resistance than SASN600 with heavy Cr depletion around grain boundary. Intergranular carbide in SN 600 is more closely spaced than that in TT 600 while thickness of the intergranualr carbide in SN 600 is smaller than that in TT 600. These results suggest that SCC resistance of Alloy 600 is given by a product of line coverage of intergranular carbide, intergrular carbide thickness and Cr concentration at grain boundary.

3.4 SCC resistance of archive materials

SCC rates of LT 600 and archive materials of HT 600 and TT 690 with an initial stress of 565 MPa tested in 10 % NaOH at 315 ℃ are shown in Fig. 2. LT 600 is most susceptible to SCC of all the materials. TT 690 exposed to 10 % NaOH for 15 days has no SCC crack. The four HT Alloy 600s showed similar SCC resistance even though the HT 600s were fabricated by three vendors. All archive HT 600s tested in 10 % NaOH showed similar SCC resistance probably due to similar microstructure and mechanical properties among them as shown in Table 3

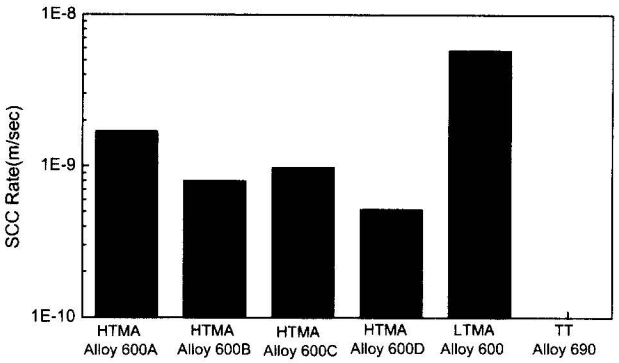

Fig. 2. SCC Rate of Staem Generator Materials in 10% NaOH at 315℃

or due to too aggressive environment to differentiate the delicate difference among them. These results are con sistent with finding by Jacko that subtle differences were observed to occur from heat to heat tested in 1 % NaOH at 316 ℃ and 343 ℃ and in 10 % NaOH at 288 ℃, 302 ℃ and 332 ℃ for a mill annealed Alloy 600 or TT Alloy 600.[15] At any rate, the accelerated test condition such as high stress, high temperature and concentrated solution narrow down the difference of SCC crack initiation time and propagation rate. No SCC was observed in 36 days tested in 1 % NaOH. LT 600 was least resistant to SCC and TT 690 was most resistant to SCC in 10% NaOH and 40% NaOH.

3.5 Effect of NaOH.

Effect of NaOH concentration on SCC of the HT 600 tested at an initial stress of 340 MPa is shown in Fig. 3. Slope of the log-log plot of SCC rate vs. NaOH concentration is about 2.4. No SCC was observed on SN 600 and TT 600 C-ring specimen with an initial stress of 340 MPa tested in 10 % NaOH for 9 days. But as shown in Table 5, significant SCC was observed on SN 600 and TT 600 with an initial stress of 565 MPa tested in 10% NaOH for 9 days. No SCC was observed after 36 days of testing in 1% NaOH at 315 ℃, in which stress at the apex of the C-ring specimen was ranging from 300 MPa to 565 MPa. Slope of the log-log plot of SCC rate vs. NaOH at 200 mV above corrosion potential was about 2.4. In this plot, SCC crack initiation period, slow SCC crack propagation stage, and fast SCC crack propagation stage were not differentiated and SCC rate was calculated by just dividing the maximum crack length with the exposure time. In addition, the slope was measured over a NaOH concentration from 10 % to 40 %. The slope measured in this work is higher than the slope of 0.66 for MA Alloy 600 and about 1 for TT Alloy 600 in slow crack growth stage reported by Vailant, et. al.[18]. In their

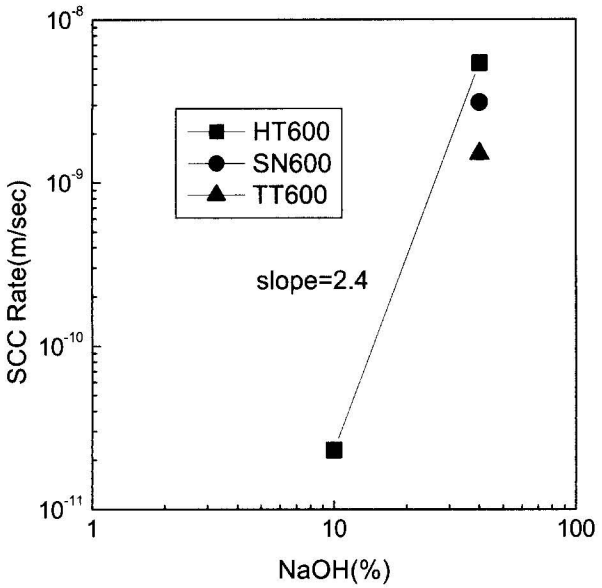

Fig. 3. NaOH concentration dependency of SCC rate at an initial stress of 340MPa and at 315℃ and at 200mV above corrosion potential.

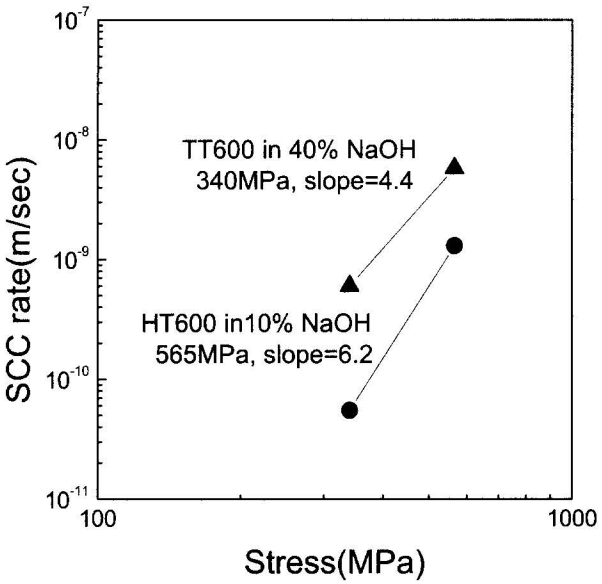

Fig. 4. Stress dependency of SCC rate.

reasoning about the slope, it is implicitly noted whether the slope is estimated for SCC at free corrosion potential or at controlled potential. The slope estimated from SCC rate vs. high temperature pH published from EPRI[19] is about 3.6 for mill annealed Alloy 600 over a pH from 10 (corresponding to 1 % NaOH) to 10.4 (corresponding to 10 % NaOH). So, the slope of 2.4, measured in this work seems to be reasonable in predicting SCC rate as a function of NaOH concentration in alkaline solution.

3.6 Effect of stress

Stress dependency of SCC rate of Alloy 600 is shown in Fig. 4. Both C-ring specimen of HT 600 and SN 600 with an initial stress of 565 MPa tested in 40 % NaOH for 10 hrs and that of HT 600 with an initial stress of 340 MPa tested in 40 % NaOH for 2 days were almost through wall cracked. So, the slope of the log-log plot of SCC rate vs. stress for HT 600 and SN 600 is not representing actual situation. The slope for TT 600 is about 4.4 in 40 % NaOH.

In primary water, the slope is in the range from 4 to 7 depending on investigator.[16),17)] Actually, those environments used in this work are too aggressive compared to primary water in a nuclear power plant. However, those results imply that SCC rate of Alloy 600 is a strong function of stress, thereby high stress which may arise from denting, and over expansion as in one of Korean nuclear power plant should be avoided.

4. Conclusion

SCC resistance of Ni-χCr-10Fe alloy increased as the Cr content of the alloy increased if the density of an intergranular carbide were comparable. SCC resistance of Alloy 600 increased in caustic solution as product of coverage of an intergranular carbide in grain boundary, intergranular carbide thickness and Cr concentration at grain boundary increased. Low temperature mill annealed Alloy 600 with small grain size and without intergranular carbide was most susceptible to SCC. TT Alloy 690 was most resistant to SCC due to high value of the product of coverage of an intergranular carbide in grain boundary, intergranular carbide thickness and Cr concentration at grain boundary. Dependency of SCC rate on stress and NaOH concentration was obtained.

Acknowledgement

This work has been done as a part of the Steam Generator Project of the Mid and Long-Term Program financially supported by the MOST in Korea.

References

1. J. P. N. Paine, S. A. Hobart, and S. G. Sawochka, in *Proceedings of the 5th International Symposium on Environmental Degradation of Materials in Nuclear Power Systems-Water Reactors*, Monterey, CA, 1991, p.739.

2. C. Goffin, J. Jadot, and L. Duvivier, in *Proceedings of International Symposium Fontevraud IV*, Fontevraud France, 1998, p.441.
3. P.M. Scott and P.Combrade, in *Proceedings of the 9th International Symposium on Environmental Degradation of Materials in Nuclear Power Systems-WaterReactors*, Amelia Island, FL,1997, p.65.
4. Korea Instutute of Nuclear Safety, *Actions for Steam generator Tube IGSCC in YoungKwang Unit 4*, 2001.
5. W. Staehle, *Basis for Predicting the Earliest Penetrations due to SCC for Alloy 600 on the Secondary Side of PWR Steam Generators*, Presented at Seminar at KAERI, Korea, 2001.
6. J. K. Sung, J. Koch, T. Angeliu, and G. S. Was, *Metall. Trans.A*, **23A**, 2887 (1992).
7. R. J. Jacko, in *Corrosion Evaluation of Thermally Treated Alloy 600 Tubing in Primary and Faulted Secondary Water Environments*, EPRI NP-6721-ISD, 1990.
8. L. E. Murr, *Interfacial Phenomena in a Metals and Alloys*, Addison Wesley Publishing Company 1975, p.145
9. P. Lin, G. Palumbo, U. Erb, and K. T. Aust, *Scripta Metallurgical Materialia*, **33**(9), 1387 (1995).
10. P. E. Doherty, D. M. Doyle, J. M. Sarver, and B. P. Miglin, in *Proceedings of a Conf. on Control of Corrosion on the Secondary Side of Steam Generators*, Airlie, Virginia, USA, 1995 p.401
11. D. C. Crawford and G. S. Was, *Met. Trans. A*, **23A**(4), 1195 (1992).
12. K. Yamanaka and J. Murayama, in *Proc. of the 4th Intern. Symp. on Environmental Degradation of Materials in Nuclear Power Systems-Water Reactors*, Georgia, USA, 1989, p.5
13. F. Vaillant, E-M Pavageau, M, Bouchcourt, J-M Boursier, and P. Lemaire, in *Proceedings of 9th International Symposium on Environmental Degradation of Materials in Nuclear Power Systems-Water Reactors*, Amelia Island, FL, 1997, p.679.
14. PWR Secondary Water Chemistry Guidelines Revision Committee, *PWR Secondary Water Chemistry Guidelines - Revision 3*, EPRI TR-102134, Revision 3, 1993.
15. R. Bandy and D. van Rooyen, *Nuclear Engineering and Design*, **86**, 49 (1985)
16. T. Yonezawa, N. Sagaguri, and K. Inimura, in *Proceedings of JAIF International Conference in Water Chemistry in Nuclear Power Plants*, Tokyo, Japan, 1988, p.490.